Biol. Cybernetics 31, 209—217 (1978)

Biological Cybernetics

An Inference upon the Neural Network Finding Binocular Correspondence*

Y. Hirai[1] and K. Fukushima[2]

[1] Institute of Information Sciences and Electronics, University of Tsukuba, Sakura-mura, Niihari-gun, Ibaragi, and
[2] NHK Broadcasting Science Research Laboratories, Kinuta, Setagaya, Tokyo, Japan

Abstract. Previously, the authors proposed a model of neural network extracting binocular parallax (Hirai and Fukushima, 1975). It is a multilayered network whose final layers consist of neural elements corresponding to "binocular depth neurons" found in monkey's visual cortex. The binocular depth neuron is selectively sensitive to a binocular stimulus with a specific amount of binocular parallax and does not respond to a monocular one. As described in the last chapter of the previous article (Hirai and Fukushima, 1975), when a binocular pair of input patterns consist of, for example, many vertical bars placed very closely to each other, the binocular depth neurons might respond not only to correct binocular pairs, but also to incorrect ones. Our present study is concentrated upon how the visual system finds correct binocular pairs or binocular correspondence. It is assumed that some neural network is cascaded after the binocular depth neurons and finds out correct binocular correspondence by eliminating the incorrect binocular pairs. In this article a model of such neural network is proposed. The performance of the model has been simulated on a digital computer. The results of the computer simulation show that this model finds binocular correspondence satisfactorily. It has been demonstrated by the computer simulation that this model also explains the mechanism of the hysteresis in the binocular depth perception reported by Fender and Julesz (1967).

1. Introduction

Hubel and Wiesel (1970) found "binocular depth neurons" in monkey's visual cortex. A binocular depth neuron is selectively sensitive to a particular orientation and position of line stimulus. It is also selectively sensitive to a specific amount of binocular parallax caused by a pair of lines with similar orientation and does not respond to a monocular stimulus. When the orientation of the line projected on the left retina deviates from that on the right retina, they cease to respond. These data suggest that, in order to yield depth perception, a binocular pair of input patterns should have almost the same orientation.

In a recent article, the authors proposed a model of neural network extracting binocular parallax (Hirai and Fukushima, 1975). It is a multilayered network whose final layers consist of neural elements corresponding to "binocular depth neurons".

When we watch a binocular pair of stimuli, each of which consists of, say, N vertical bars arranged closely to each other and is projected at the corresponding positions on both retinas, there would be $N \times N$ possible binocular pairs of vertical bars. Even in such a case, we perceive only N correct binocular pairs and all the other pairs are suppressed. So, in the brain there must be a neural network finding correct binocular pairs or "binocular correspondence".

Here we propose a model of neural network finding binocular correspondence on the assumption that some neural network is cascaded after the binocular depth neurons and determines binocular correspondence[1]. Since we have no physiological data on this point, the structure of the model is inferred from somewhat psychological and engineering points of view. To simplify the analysis, the effect of the eye movement, by which the images on both retinas are brought into fusional area, is not incorporated in this model.

The performance of the model has been simulated on a digital computer. In computer simulation, the left

* This work has been done in the NHK Broadcasting Science Research Laboratories

1 Preliminary report of this model was presented in Japanese (Hirai and Fukushima, 1976)

0340-1200/78/0031/0209/$01.80

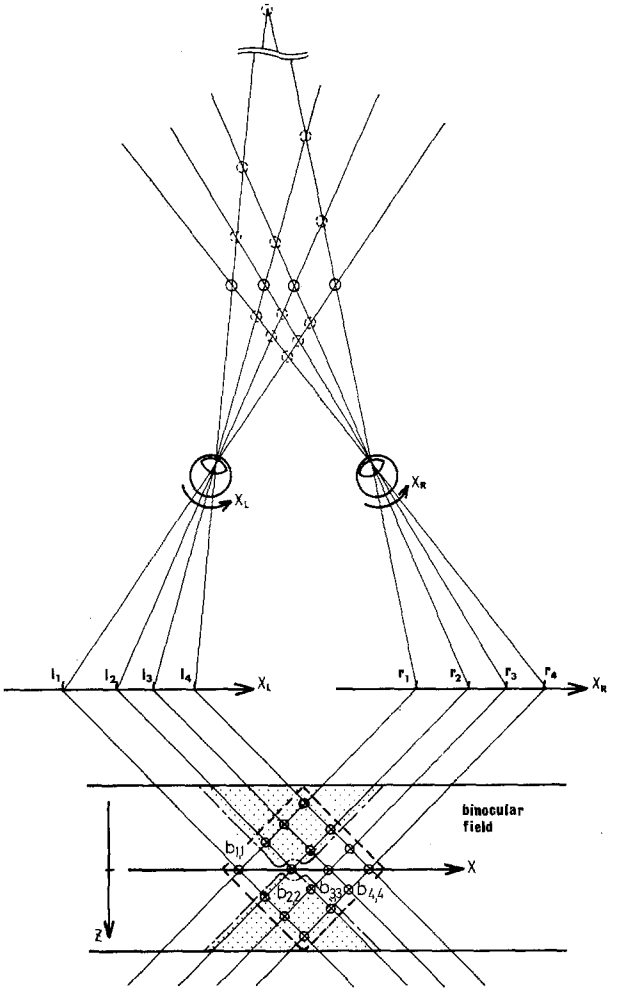

Fig. 1. A schematic diagram showing how the neural elements in the binocular field respond to a binocular input

and the right retina are assumed to be one dimensional. The results of the computer simulation show that this model can find binocular correspondence satisfactorily. It has been demonstrated by the computer simulation that this model also explains the mechanism of the hysteresis in the binocular depth perception reported by Fender and Julesz (1967).

Similar models have been proposed by Marr and Poggio (1976) and Marr et al. (1978). The differences between their models and our model are discussed in the conclusion.

2. Problem of Binocular Correspondence

Our previous model of neural network extracting binocular parallax (Hirai and Fukushima, 1975) has multilayered structure. Two input layers, corresponding to the left and the right retina, are composed of photoreceptors arranged in two-dimensional arrays. All other layers are composed of analog threshold elements also arranged in two-dimensional arrays. The neural elements of the final layers correspond to the binocular depth neurons.

Figure 1 schematically shows how the neural elements of the final layers of the previous model respond to the objects in the visual space. To simplify the illustration, only the left and the right photoreceptor layers and the final layers are illustrated. The figure shows only a group of neural elements selectively sensitive to one particular orientation of line stimulus (say, vertical bar). The neural elements of the final layers are arranged in a three-dimensional space (x, y, z). In the figure, however, to simplify the following explanations, a cross section perpendicular to y-axis, that is, (x, z) plane is presented. A neural element situated at (x, z) responds only when a binocular pair of inputs are projected at $x_L = x - z/2$ on the left retina and at $x_R = x + z/2$ on the right retina simultaneously. That is, x indicates a direction to which the binocular stimulus is seen, and z indicates binocular parallax between the left and the right retinal images. It is assumed that there is no binocular depth neuron outside a limitted range of z, that is, $|z| > z_{\max}$. The belt-zone in the (x, z) plane where the binocular depth neurons are situated is named "binocular field".

Figure 1 shows how the binocular depth neurons respond when a pattern composed of four vertical bars of small intervals is presented to both the left and the right retina. The binocular depth neurons which respond to this stimulus are situated at the intersections of the two sets of parallel lines drawn from the positions of the bars on the left and the right retina. As shown in the figure, when the intervals between the bars are narrow, every binocular pair of bars in the belt-shaped binocular field elicits a response. It is psychologically observed that when we, human being, are presented with such binocular pattern, we perceive only the binocular pairs $b_{1,1}$, $b_{2,2}$, $b_{3,3}$, and $b_{4,4}$, and do not perceive any other pairs. There is little physiological data suggesting how the binocular depth neuron or other neurons in the visual cortex respond in such a situation.

3. Basic Ideas of the Model

The structure of the neural network finding binocular correspondence is inferred from somewhat psychological and engineering points of view. It is assumed that a neural network is cascaded after the binocular depth neurons and determines binocular correspondence. It is assumed that neural network should satisfy following two basic conditions.

Condition 1. In case like Fig. 1, a stimulus l_2, for example, has a possibility to have a binocular correspondence with one of r_1, r_2, r_3, and r_4.

This condition comes from a psychological observation: When we watch such a stereopattern as shown in Fig. 1, we can perceive only the binocular pairs $[l_i, r_i]$ and all other pairs are suppressed. It is postulated that this condition is implemented by a mutually inhibitory neural network: Each neural element in the binocular field receives inhibitory inputs from neural elements whose responses are contradictory to its response. For example, as illustrated in Fig. 1, the response of the element $b_{2,2}$ is contradictory to those of the elements in the upper and lower triangular regions shown by the shading. Therefore, the element $b_{2,2}$ receives inhibitory inputs from the elements in those regions, and, at the same time, sends inhibitory signals to these elements. All neural elements in the binocular field are considered to have such mutually inhibitory connections.

Prior to the explanation of the whole model, the function of this mutual inhibition is explained in a simplified model as illustrated in Fig. 2. This figure shows a case where vertical bars are so arranged that bar A and bar F stand side by side with a small distance. It is supposed that the eyes are fixated on bar F. The mutually inhibitory connections in question are illustrated in Fig. 3. It is assumed that each neural element is analog threshold element with time lag of first order as illustrated in Fig. 4. The symbol b_i denotes the i-th neural element or its internal potential, and E_i indicates an excitatory input to that element ($i=1,2,3,4$). The output of each element is represented by $\varphi(b_i)$ where $\varphi()$ describes the nonlinear transfer characteristics of the analog threshold element, and is defined by

$$\varphi(b)=\begin{cases} b & \text{if } b>0 \\ 0 & \text{if } b\leqq 0. \end{cases} \tag{1}$$

If all coefficients of the inhibitory connections are the same and equal to w, the behavior of each element is expressed by

$$\mu\frac{db_1}{dt}+b_1=E_1-w[\varphi(b_2)+\varphi(b_3)+\varphi(b_4)], \tag{2}$$

$$\mu\frac{db_2}{dt}+b_2=E_2-w[\varphi(b_1)+\varphi(b_4)], \tag{3}$$

$$\mu\frac{db_3}{dt}+b_3=E_3-w[\varphi(b_1)+\varphi(b_4)], \tag{4}$$

$$\mu\frac{db_4}{dt}+b_4=E_4-w[\varphi(b_1)+\varphi(b_2)+\varphi(b_3)], \tag{5}$$

where μ is time constant of the neural elements.

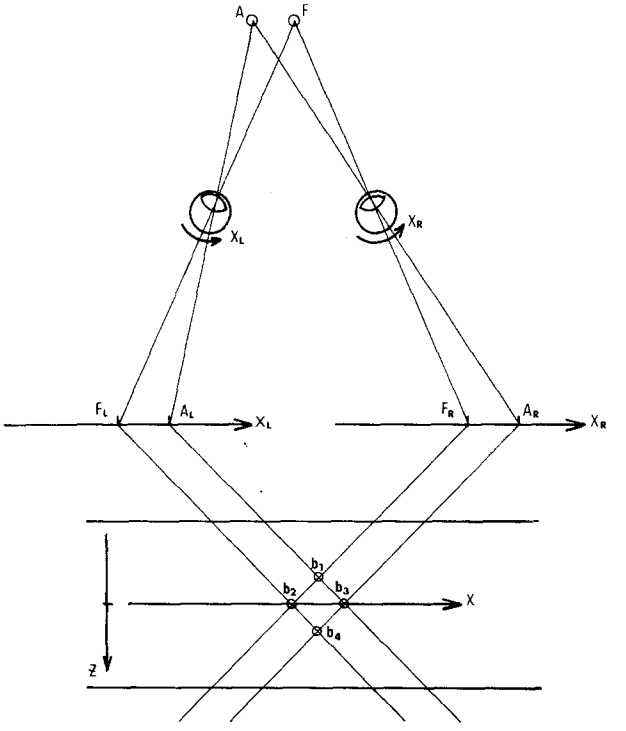

Fig. 2. An example of relation between objects in the visual space and the response of binocular field

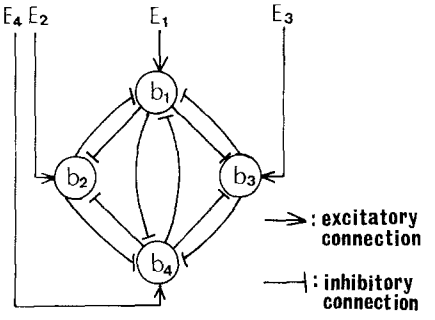

Fig. 3. Mutually inhibitory connections among neural elements in the binocular field

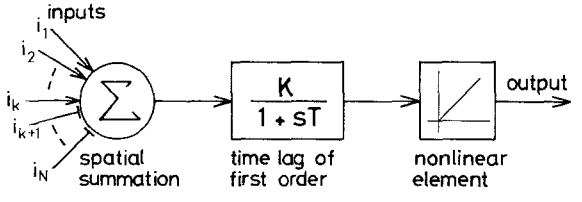

Fig. 4. A neuron model employed in the computer simulation: analog threshold element with time lag of first order

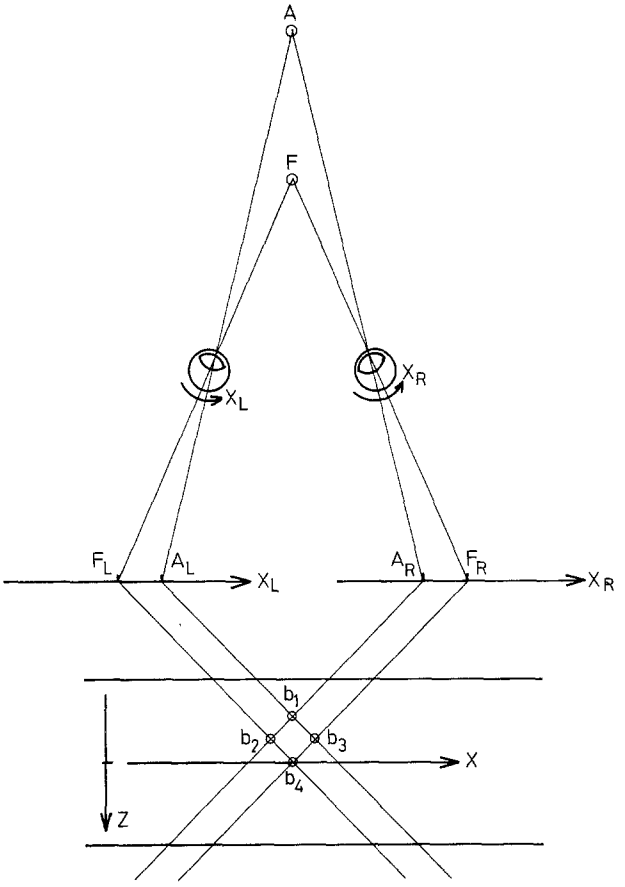

Fig. 5. Another example of the relation between objects in the visual space and the response of binocular field

Let us consider the equilibrium state of these equations. Making the derivatives $\frac{db_i}{dt}$ $(i=1,2,3,4)$ in above equations equal to zero, we obtain:

$$b_1 = E - w[\varphi(b_2)+\varphi(b_3)+\varphi(b_4)], \tag{6}$$

$$b_2 = E - w[\varphi(b_1)+\varphi(b_4)], \tag{7}$$

$$b_3 = E - w[\varphi(b_1)+\varphi(b_4)], \tag{8}$$

$$b_4 = E - w[\varphi(b_1)+\varphi(b_2)+\varphi(b_3)]. \tag{9}$$

In these equations, it is assumed that all the inputs E_i $(i=1,2,3,4)$ are equal to $E(>0)$.

When we see such vertical bars as illustrated in Fig. 2, we perceive binocular pairs b_2 and b_3, and do not perceive any other pairs, namely, b_1 and b_4. In order that the model shows the same response, the steady-state values of b_2 and b_3 are required to be positive, and those of b_1 and b_4 are required to be negative or equal to zero. Then, we obtain the following inequalities from (6)–(9)

$$b_1 = E(1-2w) \leqq 0, \tag{10}$$

$$b_2 = E > 0, \tag{11}$$

$$b_3 = E > 0, \tag{12}$$

$$b_4 = E(1-2w) \leqq 0. \tag{13}$$

It is seen from these equations that the magnitude of w should be in the range of $w \geqq 1/2$.

Near this equilibrium state, the behavior of each neural element is described by the following differential equations.

$$\mu\frac{db_1}{dt} + b_1 = E - w(b_2+b_3), \tag{14}$$

$$\mu\frac{db_2}{dt} + b_2 = E, \tag{15}$$

$$\mu\frac{db_3}{dt} + b_3 = E, \tag{16}$$

$$\mu\frac{db_4}{dt} + b_4 = E - w(b_2+b_3). \tag{17}$$

The above equations can be rewritten with vector notations as follows

$$\mu\frac{d\mathbf{b}}{dt} = \mathbf{E} - A\cdot\mathbf{b}, \tag{18}$$

where

$$A = \begin{pmatrix} 1 & w & w & 0 \\ 0 & 1 & 0 & 0 \\ 0 & 0 & 1 & 0 \\ 0 & w & w & 1 \end{pmatrix}. \tag{19}$$

Since all the eigen values of (19) have positive real part, this equilibrium state is asymptotically stable.

Another example of the response of the binocular field is illustrated in Fig. 5. This figure shows a case where vertical bars are so arranged that bar A is just behind bar F, and the eyes are fixated on bar F. Since the binocular parallax of the bar F is smaller than those of any other pairs, only the response of b_4 (corresponds to bar F) yields depth sensation. The images on the retinas A_L and A_R are perceived monocularly. Therefore, in spite of the symmetrical structure of the mutually inhibitory neural network shown in Fig. 3, only the internal potential b_4 should be positive, and b_1, b_2, and b_3 should be negative or equal to zero in the steady state. A method which makes b_4 positive and makes b_1, b_2, and b_3 negative might be to modify the excitatory inputs in such a way that E_4 be larger than E_1, E_2, and E_3. In this model, however, we employed another method. It is assumed that inhibitory inputs, namely, I_1, I_2, I_3, and I_4 are applied externally to the elements b_1, b_2, b_3, and b_4, respectively, and their magnitudes are so adjusted that I_4 becomes smaller than I_1, I_2, and I_3. Here we introduce following Condition 2 as a rule for that modification.

Condition 2. A binocular pair whose parallax is smaller than those of the others is taken as a candidate for binocular correspondence.

The Condition 2 would be reasonable, because it is psychologically observed that binocular depth perception becomes increasingly difficult with larger binocular parallax (Julesz, 1971; Sperling, 1970). Incidentally, in real life situation, we fixate an object and make its amount of binocular parallax as small as possible by the eye movement. The function of Condition 2 is implemented by modifying the inhibitory weighting coefficient to be proportional to the amount of binocular parallax.

4. Outlines of the Model

In this chapter, before the detailed explanation, the outline of the model is given. The structure of the model, together with an example of the response, is shown in Fig. 6. The model consists of three layers in all. They are named from *B* to *D*. Since only the (x, z) plane of the binocular field is considered in this article, each layer is a two-dimensional array of neural elements in the same way as the binocular field illustrated in Fig. 1.

The layer *A* corresponds to the output layers of the previous model (Hirai and Fukushima, 1975). It consists of neural elements corresponding to the binocular depth neurons, and is the binocular field itself. Each element in the *A*-layer gives excitatory signal to its corresponding elements in *B*-, *C*-, and *D*-layers. The excitatory connections from layer *A* to each of these layers are one-to-one fasion.

B-, *C*-, and *D*-layer are composed of analog threshold elements with time lag of first order. *D*-layer is the output layer of this model and transmit depth information to higher stages of the visual center. *D*-layer is composed of neural elements corresponding to excitatory neurons, and *B*- and *C*-layer are composed of neural elements corresponding to inhibitory ones.

The mutually inhibitory connections derived from Condition 1 are introduced among the neural elements of *B*-layer. The function suggested by the Condition 2 is realized by the inhibitory connections between *B*- and *C*-layer. These inhibitory connections are nearly one-to-one fashion with a slightly spreading distribution. The connections from *C*- to *B*-layer are so designed that inhibition becomes increasingly large with larger binocular parallax. The connections from *B*- to *C*-layer are constant with respect to binocular parallax.

5. Structure of the Model

5.1. A-layer

This layer corresponds to the binocular field illustrated in Fig. 1. We assume a Cartesian co-ordinate system

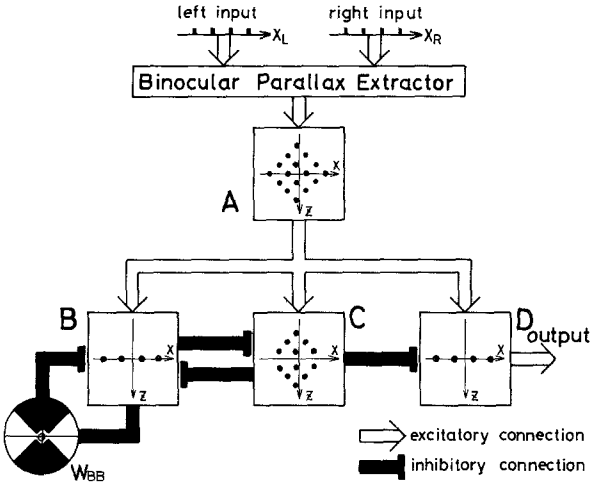

Fig. 6. Structure of the model

(x, z) on *A*-layer, and use a notation, for example, $A(x, z)$ to indicate an neural element (or output of the element) situated at point (x, z). If light stimuli are simultaneously presented at x_L on the left retina and at x_R on the right retina, only the element situated at $x=(x_L+x_R)/2$ and $z=x_R-x_L$ yields output.

The response of neural element $A(x, z)$ at time t is represented by $A(x, z, t)$. Each element of *A*-layer is assumed to yield an output represented by the following equation.

$$A(x, z, t)=\min[I_L(x-z/2, t), I_R(x+z/2, t)]. \tag{20}$$

$I_L(x, t)$ and $I_R(x, t)$ are inputs to the left and the right retina, respectively. The function min[ ] represents an operation which takes the smaller value of the two arguments.

5.2. B-layer

The response of $B(x, z)$ at time t, namely, $B(x, z, t)$, is expressed by

$$\begin{aligned} B(x, z, t)=K\cdot\varphi\Big\{\int_0^t e^{-\tau/\mu}\cdot\Big[A(x, z, t-\tau) \\ -\iint_S W_{BB}(\xi, \zeta) \\ \cdot B(x+\xi, z+\zeta, t-\tau)d\xi\cdot d\zeta \\ -W_B(z)\cdot\iint_{S'} W_{BC}(\xi, \zeta) \\ \cdot C(x+\xi, z+\zeta, t-\tau)d\xi\cdot d\zeta\Big]d\tau\Big\}, \end{aligned} \tag{21}$$

where the symbol K represents a positive constant. S and S' represent the size of the regions of *B*- and *C*-layer from which each *B*-element receives inputs. The symbol μ represents a time constant of the element. The first term of the right side of (21) represents

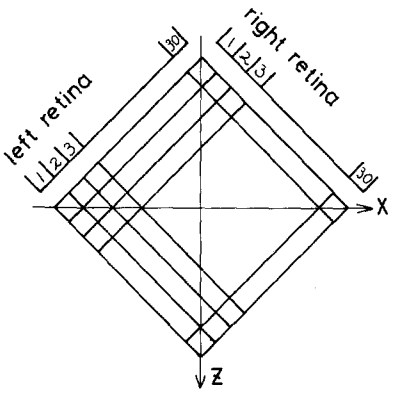

Fig. 7. A schematic diagram showing how the neural elements are arranged in a two-dimensional plane (x, z)

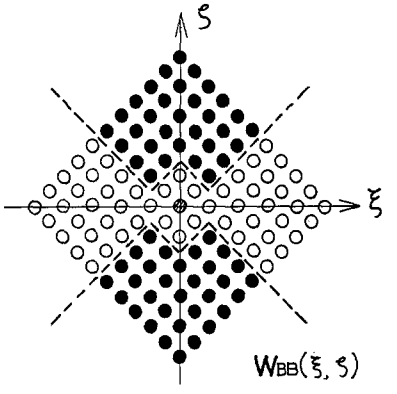

Fig. 8. Mutually inhibitory connection $W_{BB}(\xi, \zeta)$

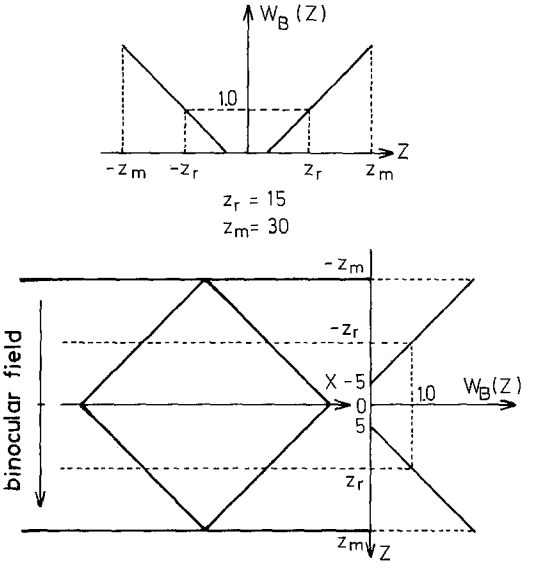

Fig. 9. Inhibitory weighting function $W_B(z)$ from C- to B-layer

an excitatory input from A-layer. The second term represents the mutually inhibitory connection within B-layer. The last term represents the inhibitory input from C-layer where $W_B(z)$ represents the weighting function of inhibition which becomes increasingly large with larger amount of binocular parallax derived from Condition 2.

5.3. *C-layer*

Each element of C-layer receives excitatory input from A-layer in one-to-one fashion, and inhibitory inputs from B-layer through the coefficient $W_{CB}(\xi, \zeta)$. The response of the element $C(x, z)$ at time t, namely, $C(x, z, t)$, is represented by

$$C(x,z,t)=K\cdot\varphi\left\{\int_0^t e^{-\tau/\mu}\cdot\left[A(x,z,t-\tau)-\iint_S W_{CB}(\xi,\zeta)\cdot B(x+\xi,z+\zeta,t-\tau)d\xi\cdot d\zeta\right]d\tau\right\}. \tag{22}$$

5.4. *D-layer*

This is the output layer of this model. Each element receives excitatory input from A-layer in one-to-one fashion, and inhibitory input from C-layer. The response of the element $D(x, z)$ at time t, namely, $D(x, z, t)$, is represented as follows

$$D(x,z,t)=K\cdot\varphi\left\{\int_0^t e^{-\tau/\mu}\cdot\left[A(x,z,t-\tau)-\iint_S W_{DC}(\xi,\zeta)\cdot C(x+\xi,z+\zeta,t-\tau)d\xi\cdot d\zeta\right]d\tau\right\}. \tag{23}$$

6. Computer Simulation of the Model

The performance of the model has been simulated on a digital computer (IBM 370/135 with 248 k-Byte core). Each retina is assumed to be one-dimensional array composed of 30 photoreceptors. Each of layers A, B, C, and D consists of 30×30 neural elements as illustrated in Fig. 7. It corresponds to the rhombic region enclosed by broken lines illustrated in Fig. 1. The time constant μ employed here is 3 ms.

6.1. *Interconnecting Coefficients between Layers*

6.1.1. $W_{BB}(\xi, \zeta)$. As illustrated in Fig. 8, the mutually inhibitory connection in B-layer, $W_{BB}(\xi, \zeta)$, is so designed that a neural element situated at the center $B(x, z)$ (indicated by ◍) inhibits the neural elements

$B(x+\xi, z+\zeta)$ indicated by the filled circles. The value of $W_{BB}(\xi, \zeta)$ in the defined region is taken as $W_{BB}(\xi, \zeta) = 2.0$.

6.1.2. $W_{CB}(\xi, \zeta)$ and $W_{DC}(\xi, \zeta)$. Each interconnecting coefficient, say, $W_{CB}(\xi, \zeta)$ is so designed that a neural element $C(x, z)$ receives inhibitory signals from 3×3 neural elements $B(x+\xi, z+\zeta)$ of B-layer centered at $B(x, z)$. The values are as follows: $W_{CB}(\xi, \zeta) = 1.01$ and $W_{DC}(\xi, \zeta) = 2.0$ in their defined 3×3 regions.

6.1.3. $W_B(z)$ and $W_{BC}(\xi, \zeta)$. The inhibitory connections from C- to B-layer are so designed that a neural element $B(x, z)$ receives inhibitory signals from 3×3 neural elements $C(x+\xi, z+\zeta)$ centered at $C(x, z)$ through the interconnecting coefficients represented by $W_B(z) \cdot W_{BC}(\xi, \zeta)$. The value of $W_{BC}(\xi, \zeta)$ is equal to 1.01 in the defined 3×3 region. The weighting function $W_B(z)$ is illustrated in Fig. 9. The values $\pm z_r$ shown in the figure represent the points of $W_B(z) = 1.0$ where the strength of inhibition from C- to B-layer becomes equal to that from B- to C-layer. The value of z_r is selected to be 15 in the computer simulation. The unit of the binocular parallax is measured by the distance between centers of adjoining photoreceptors. The parallax is taken positive or negative depending on $x_R > x_L$ or $x_R < x_L$, where x_R and x_L are the positions of the input patterns. The values $\pm z_m$ represent the maximum and the minimum value of the binocular parallax to which this model is able to respond. The value of z_m is selected to be 30 in the computer simulation.

6.2. Response of the Model

The relation between the amount of binocular parallax and the response of the model is shown in Fig. 10. The results are obtained by the computer simulation. We use a notation Z to indicate a binocular parallax of the input stimulus and a notation z to indicate a position of neural element in each layer. Figure 10a shows the case where a binocular pair with $Z = 13$ is given, and the responses of neural elements B, C, and D situated at $x = 0$ and $z = 13$ are plotted. Figure 10b and c show the cases with $Z = 15$ and $Z = 17$, respectively, and the responses of the neural elements at $z = Z$ are plotted. The ordinate represents the magnitude of the response. As is seen in Fig. 10a, when the amount of binocular parallax Z ($= 13$) is smaller than z_r ($= 15$), the D-layer-element situated at position of $z = 13$ gives positive response. On the contrally, as illustrated in Fig. 10b and c, when the amount of binocular parallax is equal to or greater than z_r, no neural element of D-layer gives response in the steady state.

Another example of the response obtained by the computer simulation is shown in Fig. 11. The magnitude of the response of a neural element is indicated by

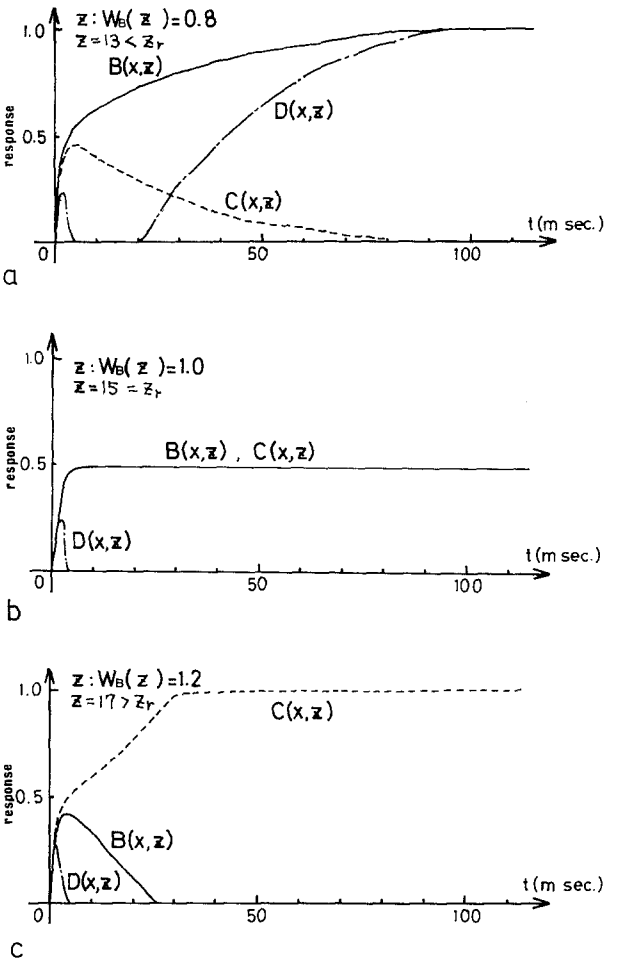

Fig. 10a–c. Responses of a neural element in each layer when a binocular input is given to the position $|Z| < z_r$ **a**, $|Z| = z_r$ **b**, and $|Z| > z_r$ **c**

the whiteness in the photographs. The input pattern is derived from a lighting spots (or vertical bars) arranged on the surface sinusoidally curved in the direction of depth. The input stimuli are presented to the 4-, 9-, 12-, 14-, 16-, 18-, 20-, 23-, and 26th element of the left retina and the 4-, 6-, 8-, 12-, 16-, 20-, 24-, 26-, and 28th element of the right retina respectively. There are 9×9 binocular pairs. As seen in the result, from 81 possible pairs this model finds binocular correspondence successfully.

These results show that this model finds binocular correspondence even in the case where the input patterns are made up by the repetition of identical pattern components, say, lighting spots with same size or vertical bars with same width and length.

7. Hysteresis in the Depth Perception

Fender and Julesz (1967) found the hysteresis phenomenon in the binocular depth perception illustrated in

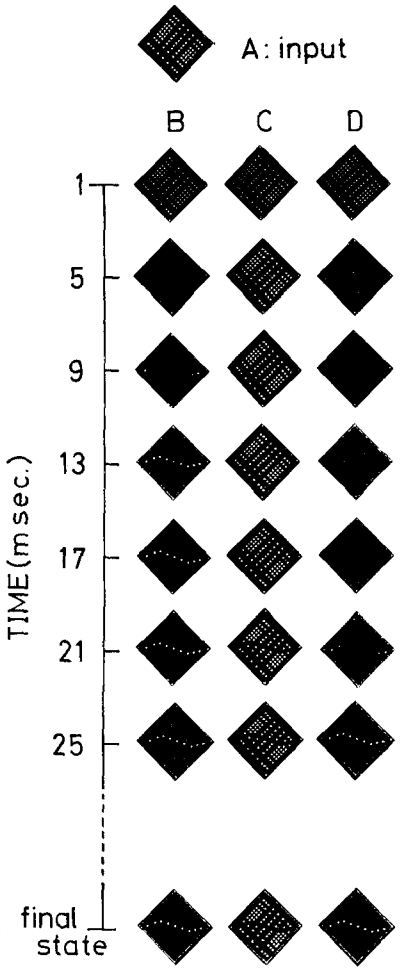

Fig. 11. An example of the response of the model

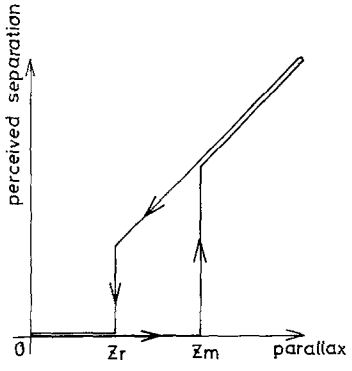

Fig. 12. Hysteresis in the binocular depth perception

Fig. 12. In the figure z_m represents the amount of binocular parallax where the fusion breaks, and z_r represents the binocular parallax where the refusion occurres. This means that a binocular pair of inputs whose parallax is smaller than z_r always fuse and yield depth sensation, but that in other case fusion and

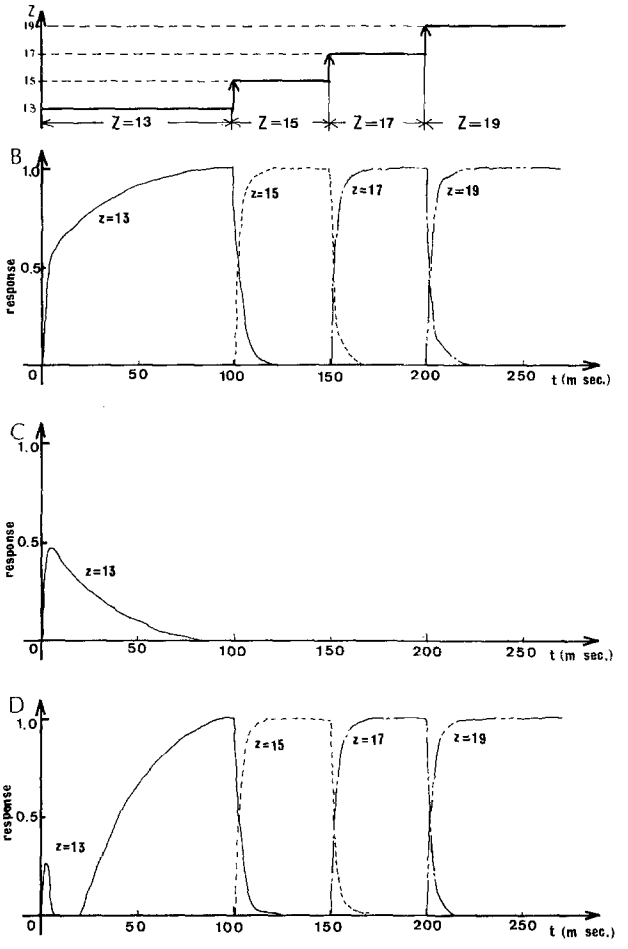

Fig. 13. An example of the response of the model showing hysteresis phenomenon

depth sensation do not always occur. The comparison with the results of Fig. 10 shows that z_r and z_m obtained psychologically correspond to those defined in this model.

An example of the response of the model showing the hysteresis in the binocular depth perception is presented in Fig. 13. In the figure, the responses of four neural elements situated at the position $z=13$, 15, 17, and 19, are shown. The amount of binocular parallax Z of the stimulus is increased from $Z=13$ ($<z_r$) to $Z=19$ ($>z_r$) with small steps. As shown in the figure, the response appears even in the case where $Z=15$, $Z=17$, and $Z=19$, while the results in Fig. 10 show that the response does not appear in such cases. In other words, when the parallax is increased slowly from $Z<z_r$ to $Z>z_r$ with small steps, the model continues to respond. When the input with a parallax $Z \geqq z_r$ is suddenly presented to the model, however, it does not respond to the stimulus. The results described above demonstrate that this model is able to explain the mechanism of hysteresis phenomenon in the binocular depth perception.

8. Conclusion

A model of neural network finding binocular correspondence has been proposed. Since we have little physiological data on this point, the structure of the model is inferred from somewhat psychological and engineering points of view. In constructing the model, it is assumed that some neural network is cascaded after the binocular depth neurons and determines binocular correspondence.

The results of the computer simulation show that this model is able to find binocular correspondence satisfactorily even in the case where the binocular input patterns are made up with the reiteration of identical picture elements such as lighting spots with the same diameter or vertical bars with the same width and length arranged on the surface curved in depth. It is also demonstrated that this model is able to explane the mechanism of hysteresis phenomenon in the binocular depth perception.

Recently, Marr and Poggio (1976) and Marr et al. (1978) proposed a cooperative stereo algorithm which satisfied the following two rules: *uniqueness* and *continuity*. In our present model *uniqueness* is implemented in a different way by the mutually inhibitory connection $W_{BB}(\xi, \zeta)$ of B-layer. *Continuity* is also, but implicitly, incorporated by $W_{BB}(\xi, \zeta)$ in a sense that a given neural element does not inhibit the others whose responses are not inconsistent with that of the given one as described in the explanation of Condition 1. Here, the meaning of *continuity* or *smoothness* is extended to include not only the neural elements with equal binocular parallax, but also all of consistent neural elements. As described above, another reasonable rule, Condition 2, is incorporated into this model.

Although only the experiments for one dimensional stereo patterns are shown in this article, this model can be extended to have a function to handle two dimensional stereo patterns, such as random-dot stereogram.

References

Fender, D.H., Julesz, B.: Extension of Panum's fusional area in binocularly stabilized vision. J. Opt. Soc. Am. **57**, 819–830 (1967)

Hirai, Y., Fukushima, K.: A model of neural network extracting binocular parallax. Biol. Cybernetics **18**, 19–29 (1975)

Hirai, Y., Fukushima, K.: An inference upon the neural network finding binocular correspondence (in Japanese). Trans. Inst. Electron. Commun. Eng. Japan **59**-D, 133–140 (1976)

Hubel, D.H., Wiesel, T.N.: Stereoscopic vision in macaque monkey. Nature **225**, 41–42 (1970)

Julesz, B.: Foundations of cyclopean perception. Chicago: The University of Chicago Press 1971

Marr, D., Poggio, T.: Cooperative computation of stereo disparity. Science **194**, 283–287 (1976)

Marr, D., Palm, G., Poggio, T.: Analysis of a cooperative stereo algorithm. Biol. Cybernetics **28**, 223–239 (1978)

Morishita, I., Yajima, A.: Analysis and simulation of networks of mutually inhibiting neurons. Kybernetik **11**, 154–165 (1972)

Sperling, G.: Binocular vision: a physical and neural theory. J. Am. Psychol. **83**, 461–534 (1970)

Received: August 8, 1978

Dr. K. Fukushima
NHK Broadcasting Science Research
Laboratories, 1-10-11, Kinuta,
Setagaya, Tokyo 157, Japan